HIGH POWER TESTS OF NORMAL CONDUCTING SINGLE-CELL STRUCTURES [*]

V.A. Dolgashev, S.G. Tantawi, C.D. Nantista , SLAC, Menlo Park, CA 94025, USA

Y. Higashi, T. Higo KEK, Tsukuba, Ibaraki 305, Japan

Abstract

We report the results of the first high power tests of single-cell traveling-wave and standing-wave structures. These tests are part of an experimental and theoretical study of rf breakdown in normal conducting structures at 11.4 GHz [1]. The goal of this study is to determine the gradient potential of normal-conducting rf-powered particle beam accelerators. The test setup consists of reusable mode converters and short test structures and is powered by SLAC's XL-4 klystron. This setup was created for economical testing of different cell geometries, cell materials and preparation techniques with short turn-around time. The mode launchers and structures were manufactured at SLAC and KEK and tested in the SLAC Klystron Test Lab.

INTRODUCTION

The accelerating gradient is one of the crucial parameters affecting the design, construction and cost of next-generation linear accelerators. The major obstacle to higher gradient is the rf breakdown. RF breakdown limits the working power and produces irreversible surface damage in high power rf components and rf sources. The recent update of the CERN based linear collider design CLIC requires 100 MV/m loaded gradient at 12 GHz in accelerating structures with heavy wakefield damping [2]. Up to now, there are no accelerators that have similar structures working at this gradient.

A major investment into the study of rf breakdown in X-band accelerating structures and rf components was made during the NLC/GLC development [3, 4, 5, 6]. Although this study advanced our understanding of the subject, many questions about the physics of rf breakdown remain unanswered. Up to now, there is no theory or simulation method that can predict breakdown performance of accelerating structures or high power rf components during their technical design. Nevertheless, NLC/GLC studies showed that breakdown behavior and breakdown characteristics such as breakdown rate *vs.* rf power and pulse length are *reproducible from structure to structure* for structures with similar geometries and rf circuits. This reproducibility gave birth to a few empirical rules that may guide the technical design and allow testing of emerging theories. Unfortunately, the well studied parameter range is narrow: X-band traveling wave (TW) structures made of copper; power up to 200 MW; $2\pi/3$ to $5\pi/6$ phase advance; and pulse length below half a microsecond. The work presented in this paper is directed toward expanding the studied parameter range with different types of structures, different materials, geometries, etc. We have manufactured ten test structures,

and at this point have tested two: one single-cell traveling-wave and one single-cell standing-wave (SW) structure. Another single-cell SW structure is under test at the time of this writing. The geometry and description of the structure/mode-launcher assemblies can be found in [1].

In our experiments, we characterize structures at a very low breakdown rate. This is similar to the way that NLC/GLC structures were tested. Here low breakdown rate means that a breakdown event happens once in a few minutes or hours when a structure is fed with pulsed rf power at 60 Hz repetition rate. During the experiment, the power and the pulse width are kept practically constant for hours. We conjecture that such experiments closely simulate the working regime of a practical accelerator. One of the results of this experiment is a map of the steady state breakdown rate *vs.* parameters of the input power pulse. We think that presenting the results in this way allows a quantitative comparison between different structures and experimental setups and let us avoid ambiguous term "breakdown limit". We note that usually during such tests the structures are continually "conditioning" and the breakdown rate slowly decrease with time. This conditioning process obviously changes the breakdown rate map. This does not prevent us from comparing different structures, since we record practically every breakdown event and can trace these changes. On the other hand, the changes are slow compared to the duration of a typical experimental run (few hours to a few days). Here experimental run means that we keep the pulse length and power practically constant while accumulating the breakdown events.

EXPERIMENTAL SETUP

The experiments are conducted at the SLAC Klystron Test Lab using a SLAC solenoid-focused XL-4 klystron. The klystron generates about 45 MW of rf power with pulse length up to 1.5 μs. For the SW structure, the power from the klystron is split: one half directed into a load, the other half through the diagnostic directional couplers into the structure. Most tests were done with a repetition rate of 60 Hz. We used two directional couplers at the input of the structure: one for measurement of the input power, another one for the reflected power. At the output of the traveling wave structure we had two other directional couplers to monitor the power transmitted through the structure and the power reflected from the high power load (the SW structure has no output coupler). We used two HP8990A peak power meters for the power measurement and crystals to measure the rf signals. We also have a photomultiplier tube (PMT) with a scintillator to monitor the dark current and breakdown-induced radiation. At the time of the SW structure testing, we added a Faraday Cup to the assembly. The signals from the crystals, PMT, and Faraday Cup

---

were measured by an Acqiris [7] digitizer. The data from the digitizer was read directly into a Widows PC using an in-house C++ code. The data from the peak power meter was read using a GPIB interface into the same computer. The peak-power meter data was continuously recorded every 2 sec. Although our code that controls the Acqiris is capable of recording every pulse, we found it impractical for the breakdown-rate experiments. Instead, all four digitizer traces are recorded for pulses with breakdowns and for pulses before and after the breakdowns. Since Windows is not a real-time system, some pulses are lost, but the number of lost pulses is small. The single-cell TW structure was installed in the Accelerator Structure Test Area (ASTA) bunker. The single-cell SW structure was installed in a lead box with 4-inch lead walls. After we realized that the PMT was saturated by dark-current-induced radiation, we used the Radical Corporation's radiation monitor 9010 to measure the integrated radiation near the structure.

RESULTS

Single-cell Travelling Wave Structure

The first single-cell TW structure tested was made at SLAC. The structure was processed to 41 MW. This was the maximum power available to the structure. This power corresponds to an accelerating gradient of 61 MV/m in the middle cell. At about a 1.2 μs pulse width there were breakdowns and outgassing in the feeding waveguide, likely at the roof of the bunker. These breakdowns prevented us from running breakdown rate experiments and getting statistically reasonable data. At this point it was clear that to test this structure we need a different power source: two klystrons combined with a pulse compressor made of the latest generation of high power components. The removable mode launcher and its critical part, a TM_{01} rf flange, worked well for at least the available power and pulse width. As with the NLC structures, the onset of X-ray radiation was at $\sim$100 MV/m peak surface electric field. Unlike in the single-cell standing-wave structure, the dark currents and the breakdown currents produced no visible damage on the vacuum viewports.

Single-cell Standing Wave Structure

The first single-cell SW structure tested was made at KEK, where it went through thorough surface processing before arriving at SLAC. It was installed inside the lead box with vacuum view ports attached to both sides of the assembly consisting of a mode launcher, the structure and pumping tees. This structure, unlike the TW structures, was processed in several hours with a small number of vacuum trips. After processing, we were able to run power into the structure almost at any level without vacuum trips from the breakdowns in the structure.

After a few days of conditioning, the setup developed a vacuum leak that was traced to the vacuum viewports. The viewport windows had become brown and had traces of discharges. We think that the windows were charged by dark currents and breakdown currents generated in the SW structure. We replaced the viewports with Faraday Cups. From that point to the end of the test period, we ran breakdown-rate experiments. Power and pulse shape were kept practically constant until a few hundred breakdowns were accumulated or there were only a few breakdowns in an 8 to 10 hour period. Then either power or pulse width were changed for the next run. Thus we have no data with less then one or two breakdowns in 8 hours. The length of each experiment was determined by the breakdown rate and lasted from a few hours to a few days. For this first structure, we accumulated more than 5,000 breakdowns over about 200 hours of klystron-on time. Usually the breakdowns generated little vacuum activity, so the klystron was not shut off after a breakdown.

The SW structure does not have a field probe inside. The on axis-field profile and the reflection from the structure were tuned using bead-pull measurements. The field inside of the structure was calculated knowing the shunt impedance of the structure and the shape of the klystron pulse. The structure should have maximum electric field of 310 MV/m for 10 MW of rf power lost in it. A periodic structure that is made with the same dimensions as the middle cell of this single-cell structure would have 2.11 times lower accelerating gradient than the maximum surface field.

To calculate the fields inside the structure, we used the input power measurements. Knowing the shape of the klystron input pulse, the structure shunt impedance and its S_{11} *vs.* frequency we calculated the time domain response of the SW structure. In this calculation we neglected the phase modulation inside the klystron pulse. Given the input power pulse we calculated the time domain fields. With those fields, we calculated the pulse heating by integrating the heat diffusion generated by rf losses [8].

We ran two series of experiments, one with standard klystron pulse (Fig. 1) and the other with a shaped klystron pulse (Fig. 2). This pulse shaping makes the field amplitude in the structure stay flat for tens of nanoseconds, thus simulating loading of the structure by a multibunch beam. Plots a) and b) in both graphs show the breakdown rate *vs.* maximum gradient in the pulse. We calculated the gradient by dividing the maximum surface electric field by 2.11. The different symbols on the graph in Fig. 1 represent different klystron pulse widths. The different symbols in Fig. 2 represent the length of the flat part of the amplitude. In this case, the klystron pulse is 100 to 200 ns longer. On the both figures the breakdowns used to generate plots a) and c) are counted differently from breakdowns for plots b) and d). On plots a) and c), all breakdowns recorded during an experimental run are shown. On plots b) and d), the breakdowns have no preceding breakdown for 17 ms, meaning no breakdown on the previous pulse. The horizontal coordinate on plots c) and d) is the maximum pulse heating temperature during the pulse (maximum temperature). In other words, this is the maximum temperature reached by the cell surface where the magnetic field is maximum (assuming linear 2D heat diffusion model). This temperature
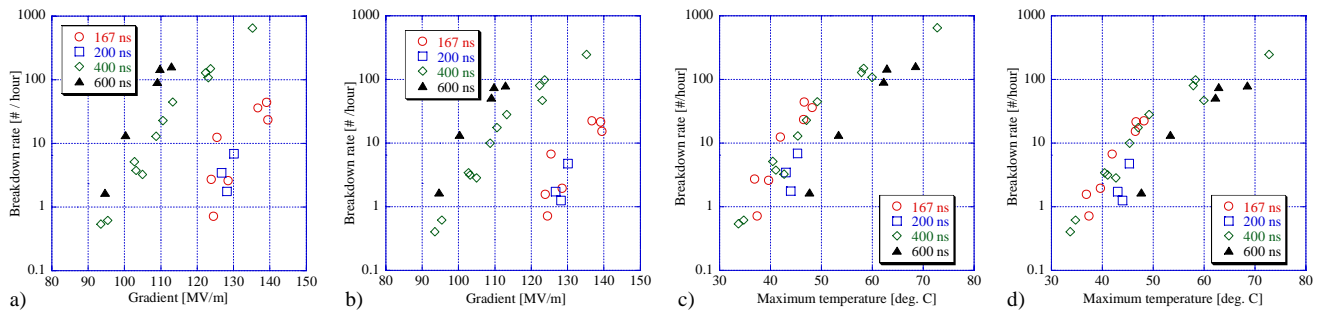
Figure 1: Breakdown rate *vs.* maximum accelerating gradient a) for all breakdowns, b) for first breakdowns, and *vs.* maximum pulse heating temperature in the structure for c) all breakdowns and d) first breakdowns. The structure is powered with "square" klystron pulse.
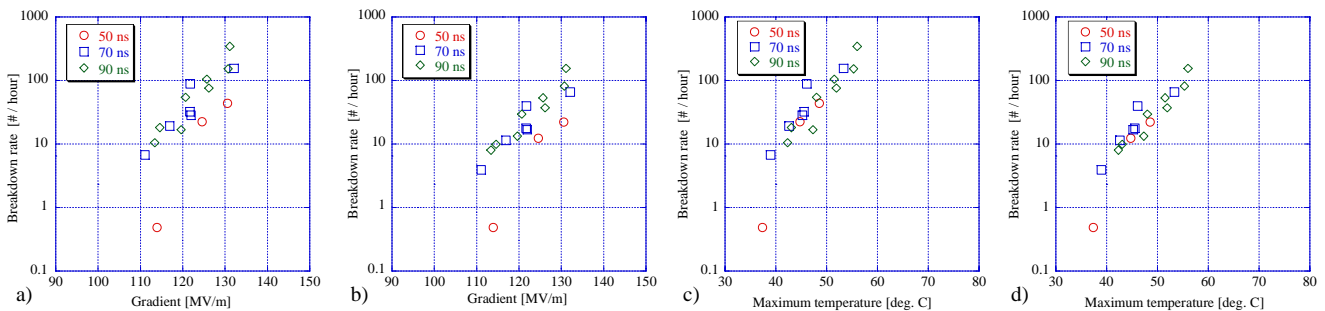

Figure 2: Breakdown rate *vs.* maximum accelerating gradient a) for all breakdowns, b) for first breakdowns, and *vs.* maximum pulse heating temperature in the structure for c) all breakdowns and d) first breakdowns. The structure is powered with modified klystron pulse so the amplitude of fields in the cavity is almost constant for 50 ns (circles), 70 ns (boxes), and 90 ns (diamonds).

is not affected by cooling of the structure. With plots c) and d), we want to show that the breakdown rate data looks more correlated if plotted *vs.* a 2D heat diffusion process (proportional to pulse heating temperature). We do not imply that this specific temperature rise is a source of the rf breakdown.

SUMMARY

With the first test of the single-cell TW structure we found that the test setup works successfully for up to 41 MW into the structure at 1.2 μs pulse length. The test was not limited by breakdowns in the structure. In the time of this publication the power source is being rebuilt in order to allow higher power.

The breakdown behavior of our first single-cell SW structure is different than the NLC/GLC TW structures and multi-cell SW structures. Unlike those structures, it protects itself – the input power is reflected from the structure after start of each breakdown. Inspite of its relatively low shunt impedance and large $a/\lambda = 2.15$, the structure ran at gradients above 110 MV/m with $\sim$ 90 ns flat top pulse (useful for acceleration of a multibunch beam) with about 10 breakdowns per hour. With "square" klystron pulse (useful for acceleration of a single bunch) the structure ran above 120 MV/m with less than one breakdown per hour.

REFERENCES

[1] V.A. Dolgashev *et al.* SLAC-PUB-11707, Proc. of PAC 2005, Knoxville, Tennessee, 595-599 (2005).

[2] Poc. of "The X-Band Accelerating Structure Design and Test-Program Workshop," CERN,Geneva, Switzerland, 18-19 June 2007.

[3] J. W. Wang, High Energy Phys. Nucl. Phys. **30**, 11 (2006).

[4] J. Wang and T. Higo, ICFA Beam Dyn. Newslett. **32**, 27 (2003).

[5] C. Adolphsen, Proc. of PAC 2003, Portland, Oregon, 668-672 (2003).

[6] V. A. Dolgashev *et al.*, Poc. of PAC03, Portland, Oregon, 1264-1266 (2003).

[7] http://acqiris.tm.agilent.com/products/digitizers.html

[8] V. A. Dolgashev, SLAC-PUB-10123, Proc. of PAC 2003, 1267-1269 (2003).